

Experimental surface-state band structure of the Si(111)-($\sqrt{3}\times\sqrt{3}$)-Au surface

C. J. Karlsson, E. Landemark, L. S. O. Johansson, and R. I. G. Uhrberg
*Department of Physics and Measurement Technology, Linköping Institute of Technology,
 S-581 83 Linköping, Sweden*
 (Received 9 July 1990)

The surface-state band structure of the Si(111)-($\sqrt{3}\times\sqrt{3}$)-Au surface has been studied in detail with polarization-dependent angle-resolved photoelectron spectroscopy. In the $\bar{\Gamma}$ - \bar{M} direction three surface states are observed, while in the $\bar{\Gamma}$ - \bar{K} - \bar{M} direction only two surface states are identified. The dispersions (initial energy versus k_{\parallel}) of these surface states have been mapped out. A nondispersive surface state, close to the Fermi level, is tentatively assigned to boundaries between $\sqrt{3}\times\sqrt{3}$ domains, which have recently been observed in scanning-tunneling-microscopy studies. It is suggested that the Fermi-level position at the surface is determined by this surface state. Comparisons with the surface electronic structure of the Si(111)-($\sqrt{3}\times\sqrt{3}$)-Ag surface show mainly differences, indicating that the Au- and Ag-induced $\sqrt{3}\times\sqrt{3}$ reconstructions have different atomic structures.

I. INTRODUCTION

The atomic and electronic structures of semiconductor surfaces with noble-metal adsorbates have attracted considerable interest recently. Both Au and Ag can induce a $\sqrt{3}\times\sqrt{3}$ reconstruction on the Si(111) surface. The atomic arrangements for these surfaces are, however, still unknown despite extensive studies. In a continuing effort to understand the complex $\sqrt{3}\times\sqrt{3}$ reconstructions, induced by Au and Ag on Si(111), we have studied the surface electronic structure of the Si(111)-($\sqrt{3}\times\sqrt{3}$)-Au ($\sqrt{3}$ -Au for short) surface in detail with polarization-dependent angle-resolved photoelectron spectroscopy (ARPES).

Two models for the atomic structure of the Si(111)-($\sqrt{3}\times\sqrt{3}$)-Au surface have been proposed. The first was proposed from an impact-collision ion-scattering spectroscopy (ICISS) study by Oura *et al.*¹ They concluded that Au triplet clusters form the reconstruction. This model requires a coverage of 1 monolayer of Au [1 monolayer (ML)= 7.8×10^{14} atoms/cm²]. A scanning-tunneling-microscopy (STM) study² and a surface x-ray-diffraction measurement³ support this model. The second model was also derived from an ICISS study, performed by Huang *et al.*⁴ but in their model the Au atoms reside at lattice sites corresponding partly to an empty honeycomb structure (70%) and partly to a centered hexagon structure (30%). The required coverage for this model would then be 0.77 ML.

Higashiyama *et al.*⁵ studied the evolution of the low-energy electron diffraction (LEED) pattern as a function of Au coverage and three different $\sqrt{3}\times\sqrt{3}$ patterns were observed: diffuse, sharp+diffuse, and sharp+ringlike spots. Higashiyama *et al.* concluded that these LEED patterns do not correspond to any well-ordered $\sqrt{3}\times\sqrt{3}$ phases. This conclusion was partially based on an earlier STM study.⁶ Another STM investigation⁷ reported dislocations on the $\sqrt{3}$ -Au surface resulting in a phase shift of $1/\sqrt{3}$ -times the 1×1 surface lattice constant between different domains. In a more detailed

STM study, by Nogami *et al.*,⁸ the $\sqrt{3}$ -Au structure is shown to consist of sub-100 Å domains separated by domain walls, corresponding to these dislocations. The $\sqrt{3}$ structure was observed for coverages between 0.8 and 0.95 ML, with a distinct decrease of the domain size for coverages larger than 0.8 ML.

A previous ARPES study⁹ along the $\bar{\Gamma}$ - \bar{K} - \bar{M} line [in the $\sqrt{3}\times\sqrt{3}$ surface Brillouin zone (SBZ), see Fig. 1(a)], reported two surface states for the $\sqrt{3}$ -Au surface. However, until now, no extensive ARPES study along both the $\bar{\Gamma}$ - \bar{K} - \bar{M} and $\bar{\Gamma}$ - \bar{M} symmetry lines has been reported. In this paper we describe the surface-state band structure of the Si(111)-($\sqrt{3}\times\sqrt{3}$)-Au surface obtained with polarization-dependent ARPES. The LEED pattern sequence reported by Higashiyama *et al.*⁵ was well reproduced in our study, except that we observed the so-called sharp+diffuse $\sqrt{3}\times\sqrt{3}$ LEED pattern for a coverage of ≈ 0.8 ML instead of 1 ML. All spectra shown in this paper were obtained from a $\sqrt{3}$ -Au surface with ≈ 0.8 ML of Au. Several surface states are observed, three in the $\bar{\Gamma}$ - \bar{M} direction and two in the $\bar{\Gamma}$ - \bar{K} - \bar{M} direction. The

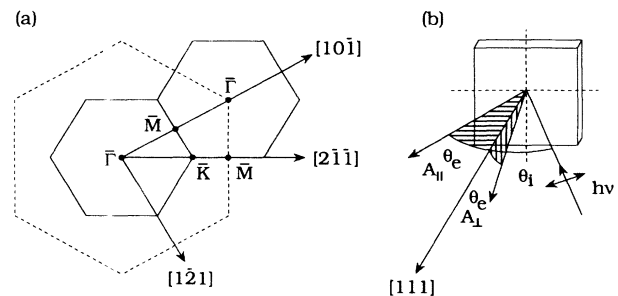


FIG. 1. (a) $\sqrt{3}\times\sqrt{3}$ and 1×1 surface Brillouin zones shown with solid and dashed lines, respectively. High symmetry points as well as bulk azimuthal directions are indicated. (b) Measurement geometries, A_{\parallel} and A_{\perp} , used in the experiment. By rotating the sample 90° around the surface normal, a given azimuthal direction can be probed with both the A_{\parallel} and A_{\perp} geometries.

dispersions, $E_i(k_{\parallel})$, of these surface states have been mapped out along the symmetry directions. One of the surface states is tentatively attributed to boundaries between $\sqrt{3}\times\sqrt{3}$ domains. It is also suggested that this surface state is responsible for the Fermi-level pinning at the surface.

II. EXPERIMENTAL DETAILS

Linearly polarized synchrotron light from the DORIS II storage ring at Hamburger Synchrotronstrahlungslabor (HASYLAB), DESY was used in the experiment, which was performed in a VG-ADES-400 spectrometer. Photoemission spectra were recorded at four different photon energies (10.2, 15, 18, and 21.2 eV). The total experimental energy resolution (monochromator and analyzer) was 0.16–0.20 eV and the angular resolution was $\pm 2^\circ$. Before insertion into the ultrahigh-vacuum chamber, the n^+ -type doped Si sample (As, 4–6 m Ω cm) was chemically precleaned and preoxidized using the Ishizaka and Shiraki method.¹⁰ *In situ* cleaning of the sample was achieved by direct current heating up to $\approx 900^\circ\text{C}$. This annealing resulted in a sharp 7×7 LEED pattern and a strong surface-state emission implying that the surface was clean and well ordered. Au atoms were evaporated onto the surface (≈ 0.8 ML) from a tungsten filament at a rate of ≈ 0.5 ML/min, as measured by a quartz microbalance. The pressure was better than 2×10^{-9} mbar during the evaporation (the base pressure of the system was $\approx 2\times 10^{-10}$ mbar). Annealing of the sample to $\approx 600^\circ\text{C}$ resulted in the so-called sharp + diffuse $\sqrt{3}\times\sqrt{3}$ LEED pattern. The Fermi-level (E_F) position was determined by photoemission from the tantalum sample holder. A work function of 4.65 eV, determined from the low-energy cutoff of the photoemission spectra, was used to obtain the $E_i(k_{\parallel})$ plots.

In order to determine the polarization dependence of the surface states, three different measurement geometries were used [see Fig. 1(b)]. In the first two cases, the photoelectrons were detected in a plane determined by the surface normal and the light polarization vector with two different light incidence angles ($\theta_i = 0^\circ$ or 45°). These cases will be referred to as A_{\parallel} geometries. The photoelectrons could also be detected in a plane perpendicular to the plane defined above. This third case will be referred to as the A_{\perp} geometry for which an incidence angle of 15° was used. By rotating the sample 90° around the surface normal, a given azimuthal direction could be probed with both the A_{\parallel} and A_{\perp} geometries.

III. RESULTS

We will limit our presentation of data to the energy range between -4 eV and E_F . At lower initial energies the dominating features are due to emission from the Au $5d$ bands. These are observed as two peaks at ≈ -4.8 and ≈ -6.8 eV relative to E_F , in agreement with the study performed by Houzay *et al.*⁹ The $5d$ peaks exhibit dispersions of approximately 0.4 eV, though the complete dispersions are difficult to determine since the $5d$ peaks coincide with structures due to direct bulk transitions for

certain k_{\parallel} values.

ARPES spectra from the $\sqrt{3}$ -Au surface recorded in the $[10\bar{1}]$ direction ($\bar{\Gamma}-\bar{M}$ in the $\sqrt{3}\times\sqrt{3}$ SBZ) for various emission angles with the A_{\parallel} geometry ($\theta_i = 45^\circ$) using 18 eV photon energy are shown in Fig. 2. Several features appear in the spectra, surface related as well as bulk related. The dispersion for the structure marked S_3 is shown in Fig. 3 together with bulk energy bands¹¹ projected onto the 1×1 SBZ (dark grey region) as well as onto the $\sqrt{3}\times\sqrt{3}$ SBZ (lighter grey region). The structure S_3 has an initial energy of 1.3 eV below E_F at $\bar{\Gamma}$ in the second $\sqrt{3}\times\sqrt{3}$ SBZ. Going towards \bar{M} it disperses downwards to a minimum at -1.7 eV and then upwards to -1.5 eV at \bar{M} . Since there is good agreement between the dispersions obtained with the four different photon energies (only 15 and 18 eV are shown in the figure), we assign S_3 to a surface state. This is further supported by

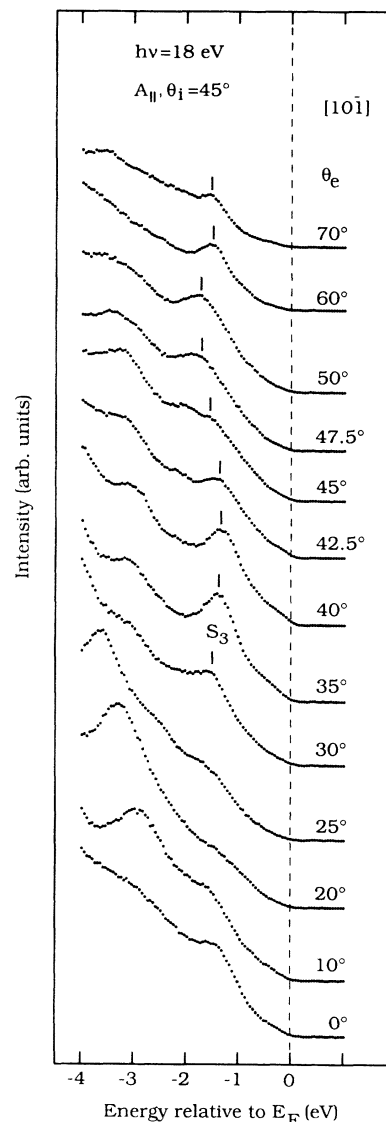


FIG. 2. ARPES spectra recorded for various angles of emission along the $\bar{\Gamma}-\bar{M}$ direction. The structure S_3 is due to emission from a surface state.

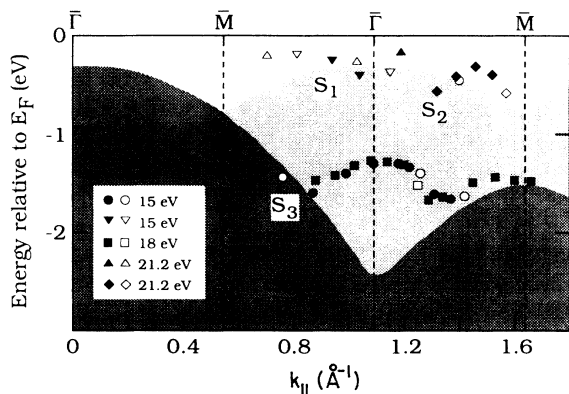


FIG. 3. Dispersions of the surface states, S_1 , S_2 , and S_3 , determined from spectra recorded in the $[10\bar{1}]$ direction. Bulk energy bands projected onto the 1×1 SBZ (dark grey region) as well as onto the $\sqrt{3} \times \sqrt{3}$ SBZ (lighter grey region) are shown. Solid symbols correspond to strong structures in the spectra; open symbols correspond to weak structures. Circles, squares, and diamonds correspond to structures in the spectra recorded using 15, 18, and 21.2 eV photon energy, respectively, with the A_{\parallel} geometry ($\theta_i = 45^\circ$). Triangles pointing down correspond to spectra recorded in the $[0\bar{1}1]$ direction with 15 eV photon energy using the A_{\parallel} geometry. Triangles pointing up correspond to spectra obtained with a photon energy of 21.2 eV and the A_{\parallel} geometry ($\theta_i = 0^\circ$).

the fact that S_3 is located in the 1×1 projected bulk band gap. The Fermi-level position at the surface for this n^+ -type doped sample is ≈ 0.3 eV above the valence-band maximum (E_V). This value for $E_F - E_V$ is obtained by comparing the initial energies of a nondispersive bulk structure in spectra, recorded with 10.2 eV photon energy, from both the $\sqrt{3}$ -Au surface and the 7×7 surface assuming that $E_F - E_V = 0.63$ eV for the 7×7 surface.^{12,13}

In Fig. 4, spectra recorded in the $[10\bar{1}]$ direction with the A_{\parallel} geometry ($\theta_i = 45^\circ$) and 21.2 eV photon energy are shown. The emission angles correspond to k_{\parallel} points in the second $\sqrt{3} \times \sqrt{3}$ SBZ where the structure marked S_2 shows the strongest emission intensity. The surface state S_3 is also seen in these spectra. S_2 is located in the $\sqrt{3} \times \sqrt{3}$ projected bulk band gap (see Fig. 3), which implies that this structure is due to emission from a surface state. The S_2 state is seen clearly only with 21.2 eV photon energy, while S_3 shows the strongest emission intensity for a photon energy of 15 eV. The highest initial energy observed for S_2 is -0.3 eV relative to the E_F . From this point it disperses steeply downwards both towards $\bar{\Gamma}$ and \bar{M} .

In order to further characterize the observed surface states, spectra were also recorded with an incidence angle of 0° (A_{\parallel} geometry). Spectra obtained in the $[10\bar{1}]$ azimuth with both $\theta_i = 45^\circ$ and 0° for an emission angle of 35° using 21.2 eV photon energy are compared in Fig. 5. The most apparent difference between the two spectra in Fig. 5 is the emission intensity close to E_F . The peak appearing almost at E_F in the $\theta_i = 0^\circ$ spectrum is due to a surface state (S_1). In this spectrum, S_1 has an initial energy of -0.2 eV relative to E_F . The dispersion of S_1

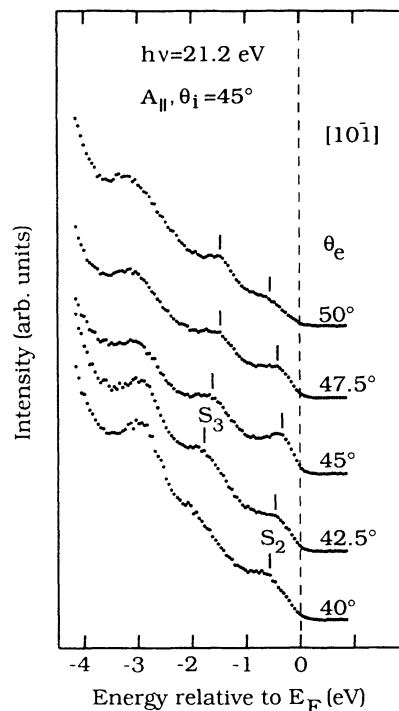


FIG. 4. ARPES spectra recorded for various angles of emission along the $\bar{\Gamma}-\bar{M}$ direction. The emission angles correspond to the k_{\parallel} region where the surface state S_2 is seen.

(shown in Fig. 3) is difficult to determine since it is seen clearly only for k_{\parallel} values close to $\bar{\Gamma}$ in the second SBZ, but it seems to be rather flat. A weak emission at the energy position of S_1 , ≈ 0.2 eV below E_F , is observed in the spectra for almost all emission angles. The spectra in Fig. 5 indicate that S_1 is excited mainly by the electric field parallel to the surface. However, in spectra at other emission angles the polarization dependence of S_1 is not at all obvious. A similar behavior is found for S_3 , i.e., the character of S_3 varies with k_{\parallel} . The emission intensity for S_2 , in the small region where it is visible, is strongly reduced when $\theta_i = 0^\circ$ is used, indicating a dominant p_z

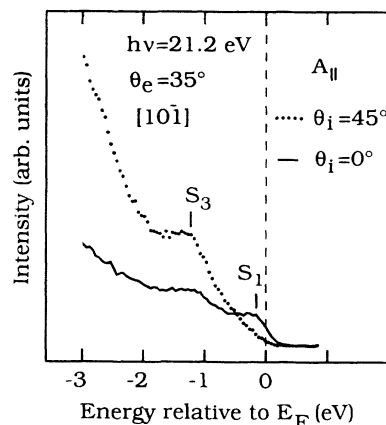


FIG. 5. ARPES spectra recorded at an emission angle of 35° and $h\nu = 21.2$ eV. The most apparent difference between the spectra recorded with $\theta_i = 45^\circ$ and 0° is the emission close to E_F , which is due to the surface state S_1 .

character for this surface state.

Spectra from the $\sqrt{3}$ -Au surface obtained in the $[2\bar{1}\bar{1}]$ direction ($\bar{\Gamma}-\bar{K}-\bar{M}$ in the $\sqrt{3}\times\sqrt{3}$ SBZ) using 18 eV photon energy are shown in Fig. 6. These spectra were recorded with the A_{\parallel} geometry and an incidence angle of 45° . The dispersions obtained for the structures marked S'_2 and S'_3 are shown in Fig. 7 together with bulk energy bands¹¹ projected onto the 1×1 and $\sqrt{3}\times\sqrt{3}$ SBZ's. The complete dispersion of S'_2 cannot be determined from the 18 eV spectra. However, in spectra recorded with a photon energy of 15 eV in the $[\bar{1}\bar{2}\bar{1}]$ direction with the same measurement geometry (shown in Fig. 8) the dispersion of S'_2 is visible. As can be seen in Fig. 7, the dispersions of S'_2 and S'_3 seem to coincide at \bar{K} at an initial energy of -1.2 eV relative to E_F . Further out in the SBZ (along $\bar{K}-\bar{M}-\bar{K}$) it is impossible to separate S'_2 and S'_3 or even to determine whether it is one or two surface states. However, enhanced emission at higher energies than -1.2 eV for k_{\parallel} along $\bar{K}-\bar{M}-\bar{K}$ may indicate that one of the surface states disperses upwards from \bar{K} . Even though there exists some ambiguity concerning the assignment of the strong surface structure along $\bar{K}-\bar{M}-\bar{K}$, it

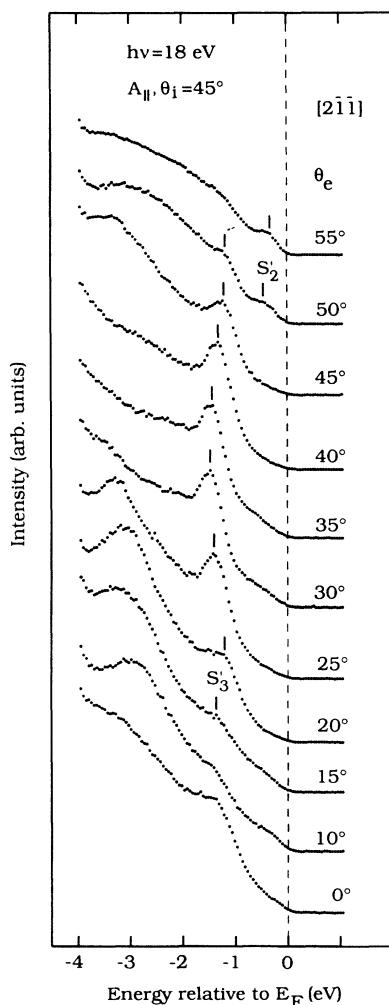


FIG. 6. ARPES spectra recorded for various angles of emission along the $\bar{\Gamma}-\bar{K}-\bar{M}$ direction. The structures S'_2 and S'_3 are interpreted as due to surface-state emission.

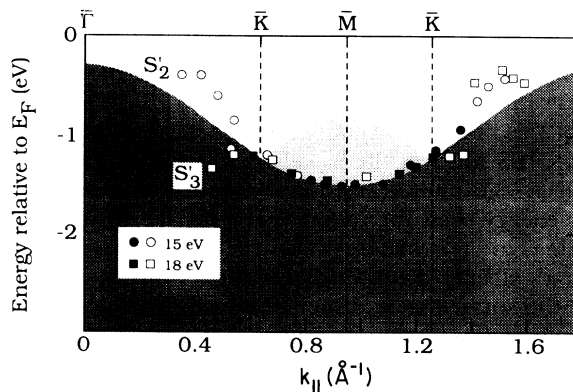


FIG. 7. Dispersions of the surface states S'_2 and S'_3 , determined from spectra recorded in the $[2\bar{1}\bar{1}]$ and $[\bar{1}\bar{2}\bar{1}]$ directions. For details, see Fig. 3.

is denoted S'_3 in the remainder of the paper. From the maximum at \bar{K} the structure S'_3 disperses downwards both towards $\bar{\Gamma}$ and \bar{M} . At \bar{M} the initial energy is -1.5 eV. Between \bar{K} and \bar{M} the dispersion of S'_3 seems to follow the 1×1 projected valence-band edge. This makes an assignment of S'_3 to a surface state somewhat uncertain. It is therefore important to point out that the energy of the valence-band edge at \bar{M} from the calculation (-1.25 eV relative to E_V) is too high compared to experimental determinations which give a \bar{M} energy of ≈ -1.5 eV relative to E_V .^{14,15} This corresponds to a \bar{M} energy of -1.8 eV relative to E_F in this study and therefore the structure S'_3 really lies in the 1×1 bulk band gap. The good agreement between the dispersions obtained with the four different photon energies (only 18 and 15 eV are shown in Fig. 7) gives further support to the surface-state interpretation of S'_3 .

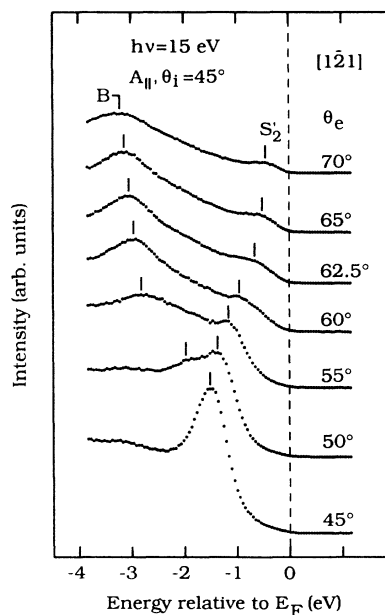


FIG. 8. ARPES spectra recorded for various angles of emission along the $\bar{\Gamma}-\bar{K}-\bar{M}$ direction showing the dispersion of S'_2 .

The most dominating feature in the spectra in Fig. 8 is the surface structure at the emission angle of 45° . At this emission angle this surface state almost coincides with a structure due to a direct bulk transition (B). The dispersion of this bulk transition has been determined in an earlier ARPES study of the Si(111) 2×1 surface.¹⁵ In the 45° spectrum the bulk transition B occurs at a somewhat lower energy than the initial energy of the surface state, resulting in a broadening of the peak. Structure B disperses steeply downwards for higher emission angles, while the surface state disperses upwards. The structure S'_2 seems to have a maximum in energy between $\bar{\Gamma}$ and \bar{K} at -0.3 eV (see Fig. 7). From this maximum it disperses downwards to -1.2 eV at \bar{K} . S'_2 is located in the projected bulk band gap which makes an assignment of S'_2 to a surface state certain.

The polarization dependence of the surface states has been investigated. Both S'_2 and S'_3 are visible with the A_{\parallel} geometries, but not when the A_{\perp} geometry was employed. This indicates that the surface may have a mirror plane containing the surface normal and the $[2\bar{1}\bar{1}]$ azimuth. By using mirror-plane selection rules,¹⁶ the symmetry of the surface states may be determined. The initial states are either even or odd under reflection in a mirror plane. Therefore, by using the A_{\parallel} (A_{\perp}) geometry, odd (even) states are suppressed. The observed polarization dependence of S'_2 and S'_3 indicates then that these surface states are both even. In contrast, the S_1 , S_2 , and S_3 surface states, in the $[10\bar{1}]$ direction, are visible with both the A_{\parallel} and A_{\perp} geometries, indicating the absence of mirror-plane symmetry in this direction. The observed polarization dependence of the surface states thus indicates that the surface reconstruction has the same symmetry as the ideal, unreconstructed surface.

IV. DISCUSSION

In the $\bar{\Gamma}-\bar{K}-\bar{M}$ direction, Houzay *et al.*⁹ assigned two structures in their spectra to surface states on the $\sqrt{3}$ -Au surface, one of which exhibits a dispersion in agreement with the dispersion determined in this study for the S'_3 surface state along $\bar{K}-\bar{M}-\bar{K}$. The dispersion determined by Houzay *et al.* between $\bar{\Gamma}$ and \bar{K} for this surface state seems somewhat uncertain since it appears only as a shoulder in their spectra and also because bulk structures could interfere with the shoulders in the spectra. The second surface structure observed in this earlier study appears as a shoulder centered around ≈ -2.9 eV in their spectra, recorded with a photon energy of 21.2 eV. This structure is observed in our study as well, but the dispersion is very hard to determine since it is a very weak structure in the 21.2 eV spectra and also since it coincides with direct bulk transitions for certain k_{\parallel} values. We observe some structures in the same energy region in the spectra recorded with the other photon energies. But it is not possible to positively identify these structures as due to a surface state (resonance) since the dispersion seems to be photon energy dependent and also since the initial energies overlap with projected bulk bands.

The surface-state band structure, determined in this study, for the $\sqrt{3}$ -Au surface shows some similarities but

mostly differences compared to the surface-state band structure for the $\sqrt{3}$ -Ag surface.¹⁷ The number of surface states in the different azimuths are the same for the two surfaces. A surface state which shows qualitative as well as quantitative agreement with the dispersion of the S_3 surface state on the $\sqrt{3}$ -Au surface was also observed on the $\sqrt{3}$ -Ag surface. The other surface states show little or no resemblance, considering dispersions as well as polarization dependences. The $\sqrt{3}$ -Ag surface has a mirror plane containing the $[2\bar{1}\bar{1}]$ azimuth, which may also be the case for the $\sqrt{3}$ -Au surface. However, on the $\sqrt{3}$ -Au surface the two surface states seem to be even, but on the $\sqrt{3}$ -Ag surface they have different symmetries in the mirror plane. These comparisons of the surface electronic structures suggest that the atomic structures for the two surfaces are different, which also must be the conclusion considering the STM images from the two surfaces. One major difference between STM images obtained from the $\sqrt{3}$ -Au and $\sqrt{3}$ -Ag (Refs. 18 and 19) surfaces is that one and two protrusions are seen per $\sqrt{3} \times \sqrt{3}$ unit cell, respectively. For the $\sqrt{3}$ -Au surface these protrusions form a hexagonal pattern, while for the $\sqrt{3}$ -Ag surface they form a honeycomb pattern. A second major difference in the images obtained from the two surfaces is the domain walls on the $\sqrt{3}$ -Au surface observed in the STM study by Nogami *et al.*⁸ In the image presented by these authors, obtained with $V_{\text{tip}} = +0.2$ V, which shows filled electron states between E_F and -0.2 eV, the dominant contribution to the tunneling current comes from the domain walls. There is also a weaker contribution, to the $+0.2$ V image, from the protrusions forming the $\sqrt{3} \times \sqrt{3}$ domains. Our ARPES measurements suggest that three surface states can contribute to this image. The surface state S_1 lies certainly in the energy range for tunneling to the $V_{\text{tip}} = +0.2$ V image. But, also the surface states S_2 , S'_2 have initial energies within the possible energy range considering the experimental uncertainty. A distinction between the origins for these surface states can be made considering that a surface state originating from the domain walls would be expected to exhibit no or a very small dispersion due to the lack of long-range order. Therefore, the non-dispersive character of S_1 , which is in contrast to the steep dispersions exhibited by S_2 , S'_2 , justifies the description of S_1 as domain-wall-related. The weaker tunneling from the domains may then originate from the steeply dispersing S_2 , S'_2 surface states.

The Fermi-level position in the bulk band gap at the $(\sqrt{3} \times \sqrt{3})$ -Au surface for an n -type doped sample (2–10 Ω cm) has been determined using Si $2p$ core-level photoelectron spectroscopy.²⁰ A shift in the Fermi-level position of ≈ 0.3 eV toward the valence band for the $\sqrt{3}$ -Au surface compared to the Si(111) 7×7 surface was observed in that study. Using a value of 0.63 eV for $E_F - E_V$ for the 7×7 surface,¹² one obtains a value of 0.33 eV for $E_F - E_V$ for the $\sqrt{3}$ -Au surface on this n -type doped sample. The observed values for $E_F - E_V$ are thus almost the same for both the n -type doped and n^+ -type doped samples. As can be seen in Fig. 5, the Fermi level cuts through the high-energy side of the structure S_1 . A very

similar situation is found on the Si(111)7×7 surface, which is metallic. The 7×7 surface also has a non-dispersing surface state at ≈ -0.2 eV relative to E_F (Ref. 21) with a finite emission intensity at the Fermi level. Therefore, it seems likely that S_1 is responsible for the Fermi-level pinning at the surface. We have suggested here, by comparing our photoemission data with the results of a STM study, that the S_1 state should be associated with the domain walls between different $\sqrt{3}\times\sqrt{3}$ areas. With this assignment of S_1 one would, in general, expect to find a laterally inhomogeneous band bending on the surface, which would depend, among other things, on the distance between the domain walls. Such lateral variations of the E_F position, if present, are estimated to be small since no apparent broadening of the bulk structures

were observed in the photoemission spectra.

In summary, the surface-state band structure of the $\sqrt{3}$ -Au surface has been determined using ARPES. Three surface states are visible in the $\bar{\Gamma}$ - \bar{M} direction, while only two surface states are observed in the $\bar{\Gamma}$ - \bar{K} - \bar{M} direction. We have tentatively assigned the nondispersing surface state, close to the Fermi level, to domain walls on the $\sqrt{3}$ -Au surface. This surface state is most likely responsible for the Fermi-level pinning at the surface.

ACKNOWLEDGMENTS

The assistance of the staff at HASYLAB is gratefully acknowledged. This work was supported by the Swedish Natural Science Research Council.

-
- ¹K. Oura, M. Katayama, F. Shoji, and T. Hanawa, *Phys. Rev. Lett.* **55**, 1486 (1985).
- ²Ph. Dumas, A. Humbert, G. Mathieu, P. Mathiez, C. Mouttet, R. Rolland, F. Salvan, F. Thibaudau, and S. Tosch, *Phys. Scr.* **38**, 244 (1988).
- ³R. Feidenhans'l, F. Grey, J. Bohr, M. Nielsen, and R. L. Johnson, *J. Phys. (Paris) Colloq.* **50**, 175 (1989).
- ⁴J. H. Huang and R. S. Williams, *Phys. Rev. B* **38**, 4022 (1988).
- ⁵K. Higashiyama, S. Kono, and T. Sagawa, *Jpn. J. Appl. Phys. Pt. 2* **25**, L117 (1986).
- ⁶F. Salvan, H. Fuchs, A. Baratoff, and G. Binnig, *Surf. Sci.* **162**, 634 (1985).
- ⁷T. Hasegawa, K. Takata, S. Hosaka, and S. Hosoki, *J. Vac. Sci. Technol. A* **8**, 241 (1990).
- ⁸J. Nogami, A. A. Baski, and C. F. Quate, *Phys. Rev. Lett.* **65**, 1611 (1990).
- ⁹F. Houzay, G. M. Guichard, A. Cros, F. Salvan, R. Pinchaux, and J. Derrien, *J. Phys. C* **15**, 7065 (1982).
- ¹⁰A. Ishizaka and Y. Shiraki, *J. Electrochem. Soc.* **133**, 666 (1986).
- ¹¹K. C. Pandey, *Phys. Rev. B* **14**, 1557 (1976).
- ¹²F. J. Himpsel, G. Hollinger, and R. A. Pollak, *Phys. Rev. B* **28**, 7014 (1983).
- ¹³C. J. Karlsson, E. Landemark, L. S. O. Johansson, U. O. Karlsson, and R. I. G. Uhrberg, *Phys. Rev. B* **41**, 1521 (1990).
- ¹⁴F. J. Himpsel, P. Heimann, and D. E. Eastman, *Phys. Rev. B* **24**, 2003 (1981).
- ¹⁵R. I. G. Uhrberg, G. V. Hansson, U. O. Karlsson, J. M. Nicholls, P. E. S. Persson, S. A. Flodström, R. Engelhardt, and E. -E. Koch, *Phys. Rev. B* **31**, 3795 (1985).
- ¹⁶J. Hermanson, *Solid State Commun.* **22**, 9 (1977).
- ¹⁷L. S. O. Johansson, E. Landemark, C. J. Karlsson, and R. I. G. Uhrberg, *Phys. Rev. Lett.* **63**, 2092 (1989).
- ¹⁸E. J. van Loenen, J. E. Demuth, R. M. Tromp, and R. J. Hamers, *Phys. Rev. Lett.* **58**, 373 (1987).
- ¹⁹R. J. Wilson and S. Chiang, *Phys. Rev. Lett.* **58**, 369 (1987); **59**, 2329 (1987).
- ²⁰U. O. Karlsson and R. I. G. Uhrberg, unpublished.
- ²¹R. I. G. Uhrberg, G. V. Hansson, J. M. Nicholls, P. E. S. Persson, and S. A. Flodström, *Phys. Rev. B* **31**, 3805 (1985).

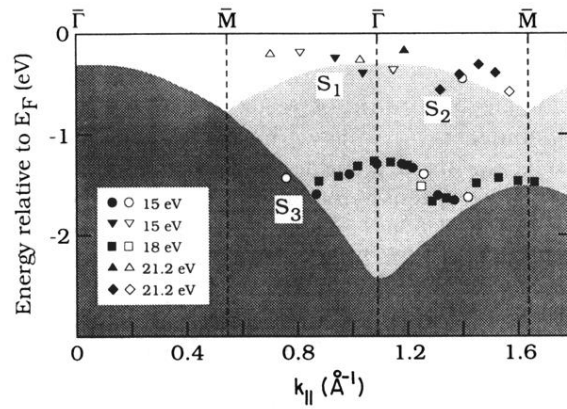


FIG. 3. Dispersions of the surface states, S_1 , S_2 , and S_3 , determined from spectra recorded in the $[10\bar{1}]$ direction. Bulk energy bands projected onto the 1×1 SBZ (dark grey region) as well as onto the $\sqrt{3} \times \sqrt{3}$ SBZ (lighter grey region) are shown. Solid symbols correspond to strong structures in the spectra; open symbols correspond to weak structures. Circles, squares, and diamonds correspond to structures in the spectra recorded using 15, 18, and 21.2 eV photon energy, respectively, with the A_{\parallel} geometry ($\theta_i = 45^\circ$). Triangles pointing down correspond to spectra recorded in the $[0\bar{1}1]$ direction with 15 eV photon energy using the A_{\perp} geometry. Triangles pointing up correspond to spectra obtained with a photon energy of 21.2 eV and the A_{\parallel} geometry ($\theta_i = 0^\circ$).

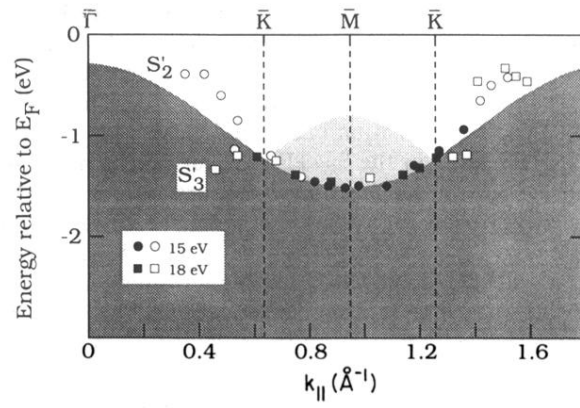


FIG. 7. Dispersions of the surface states S_2' and S_3' , determined from spectra recorded in the $[2\bar{1}\bar{1}]$ and $[1\bar{2}1]$ directions. For details, see Fig. 3.